INTERNATIONAL JOURNAL OF ENERGY STUDIES

e-ISSN: 2717-7513 (ONLINE); homepage: https://dergipark.org.tr/en/pub/ijes

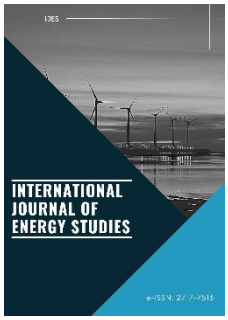

Research Article

Int J Energy Studies 2024; 9(1): 21-42

DOI: 10.58559/ijes.1429413

Received : 31 Jan 2024

Revised : 12 Feb 2024

Accepted : 12 Feb 2024

Investigation of the performance of cathode supported solid oxide fuel cell with energy and exergy analysis at different operating temperatures

Serdar Halis[a*], Nisa Nur Atak[b], Battal Doğan[c]

[a]Pamukkale University, Faculty of Technology, Department of Automotive Engineering, Denizli, Türkiye, ORCID:0000-0002-6099-7223

[b]Gazi University, Faculty of Technology, Department of Energy Systems Engineering, Ankara, Türkiye, ORCID:0009-0002-0523-6146

[c]Gazi University, Faculty of Technology, Department of Energy Systems Engineering, Ankara, Türkiye, ORCID:0000-0001-5542-4853

*(*Corresponding Author: shalis@pau.edu.tr)*

Highlights

- The performance analysis of a cathode-supported SOFC was conducted with exergy and energy analysis.
- The power density and cell potential were calculated for different operating temperature.
- The maximum exergy efficiency was determined as 66.93%.
- The maximum thermal efficieny was calculated as 71.35%.

You can cite this article as: Halis S, Atak NN, Doğan B. Investigation of the performance of cathode supported solid oxide fuel cell with energy and exergy analysis at different operating temperatures. Int J Energy Studies 2024; 9(1): 21-42.

ABSTRACT

In this research, the performance analysis of a cathode-supported solid oxide fuel cell (SOFC) with an active cell area of 0.0834 m^2 and a cathode thickness of 750 µm was carried out under three different operating temperatures (973 K, 1073 K and 1173 K). The power density and cell potential were calculated by determining the losses in the cell at 8 different current densities (1500 A/m^2 - 5000 A/m^2) for each operating temperature. It was observed that ohmic losses in SOFC have a lower effect on the cell potential compared to other losses. An increase of the operating temperature by 100 K resulted in a decrease in ohmic losses of 3.36×10^{-8} V under constant current density (CD). In addition, the rise in CD negatively affected all the losses in the cell and decreased the cell voltage. The exergy and energy analysis of SOFC was carried out by calculating the thermal efficiency, exergy destruction, entropy production and exergy efficiency for various operating parameters. An increment of 200 K in the operating temperature increased the thermal efficiency by approximately 2 times at a CD of 5000 A/m^2. Also, the minimum entropy production was obtained at an operating temperature of 1173 K and a CD of 1500 A/m^2. In this case, the entropy production was calculated as 2.63 kW/K, resulting in a maximum exergy efficiency of 66.93%.

Keywords: SOFC, Cell potential, Performance analysis, Entropy production, Exergy efficiency, Thermal efficiency

1. INTRODUCTION

Growing environmental problems and the inefficient use of energy resources are a crucial challenge for humanity at present. Therefore, the development of sustainable, efficient and clean technologies is critical to increase environmental sustainability and better utilization of energy. These technological solutions not only aim to protect nature by reducing environmental impacts, but also serve the goal of creating a sustainable world for future generations by using energy resources more efficiently. The development and adoption of clean, sustainable and effective technologies are an important initial step in the reduction of environmental problems on a global scale [1]. One of the most effective instruments in the transition to this process is fuel cells. The fuel cell is a type of electrochemical apparatus that directly produces electrical energy from the chemical energy of an oxidizing agent and a fuel. Fuel cells offer several advantages over technologies based on conventional combustion, including higher efficiency, lower or zero emissions, and the ability to use a wide range of fuels [2]. An electrolyte, a cathode and an anode are the three fundamental parts of a fuel cell. The most common types of fuel cells use hydrogen [3,4] as the fuel, although other fuels like methanol [5], ethanol [6] and carbon fuels [7] can also be utilized in various types of fuel cells. One type of fuel cell that uses solid ceramic material as the electrolyte is the solid oxide fuel cell (SOFC). The SOFC's basic working principle of involves the electrochemical reaction between oxygen ions and fuel ions across the solid electrolyte. The solid oxide electrolyte allows the cell to work at high temperatures (600-1000°C) [8]. This high operating temperature range is a characteristic feature of SOFCs. It also provides advantages such as high electrical efficiency, flexibility to be used with many different fuels [9–11] and the ability to capture and utilize waste heat, making SOFCs suitable for combined heat and power applications [12,13]. However, managing the high operating temperatures and ensuring long-term durability of materials are challenges associated with SOFC technology [14]. Nevertheless, there have been many recent studies to overcome these challenges [15–17]. As mentioned, researchers are endeavoring to investigate both hydrogen and alternative materials and fuels to achieve high efficiency [7,18–22]. The most commonly used of these fuels is hydrogen for SOFCs. The utilization of hydrogen in SOFCs shows potential for high efficiency and performance, but it also requires addressing challenges related to cost, fuel availability, and the development of alternative hydrogen carriers. Ongoing research and testing are focused on optimizing the utilization of hydrogen in SOFCs to maximize their potential as a clean and efficient energy technology. An investigation was conducted into the impact of anodic gas recirculation on the a hydrogen-fueled SOFC system's performance with the goal of optimizing this technology for use in renewable energy

storage [23]. The numerical simulation results showed that a layout with more than 80% anode gas recirculation achieved higher electrical efficiency (about 68.0%) with low flue gas fuel utilization. In addition, the fact that the high heating value (HHV) of hydrogen can reach up to 141.9 MJ shows that more energy value is released than the energy value obtained with the use of other fossil fuels other than nuclear energy [24]. When the literature is examined, it is stated that a system efficiency of approximately 49.0% is achieved in SOFCs operated with hydrogen [25]. In studies [26,27] comparing SOFC systems using hydrogen and methane fuels, it was observed that when pure hydrogen was used, the efficiency values of the system could be up to 49.0% and 44.4%, respectively, depending on the lower heating value of hydrogen. Furthermore, some studies were carried out to assess the capacity of SOFCs using biogas. Jia et al. [28] reported that the net efficiency of a SOFC system powered by biogas feeding was calculated to be about 28.0-29.0%. In a study by Papurello et al. [29] it was concluded that a SOFC plant supplied with biogas from organic wastes can achieve an electrical efficiency of about 34.0% at a usage factor of about 55.0%. In a research performed to determine the electrical efficiency of a SOFC plant using biogas from wastewater treatment plants, it was stated that the electrical efficiency of the plant reached approximately 41.0% at a usage factor of 65.0% [30]. It was also observed that the electrical efficiency of a SOFC plant using methanol as fuel was calculated to be approximately 55% [31]. In a study [32], the electrical efficiency of a plant using di methyl ether and methanol fuels was reported to be about 50%. In another SOFC plant using bioethanol, electrical efficiency was found to be as high as 53% [33]. In addition to the performance analyzes on SOFC efficiencies according to different fuel usage, energy and exergy analyzes were also conducted on SOFC systems to determine their usability depending on these efficiencies. Baniasadi and Dincer [34] evaluated the exergy and energy analysis of a combined heat and power system using an ammonia-fed SOFC with heat recovery option. When heat recovery is considered, the exergy efficiency of the system changed in the range of 60-90% while the energy efficiency was calculated at 40-60%. Since the optimum operating conditions could not be fully determined in a study [35] considering the energy analysis of a hybrid system including SOFC, energy and exergy analyses of this hybrid system were conducted to assess the load flexibility of this hybrid fuel cell system and to determine the operating conditions that will ensure stable operation of the system. In this study, it is stated that the proposed system shows good performance for power variation up to about 60% normal load distribution. In order to prevent external heat and reach a longer discharge duration, a power variation of 50%, a gas turbine pressure ratio of 2 and a charge ratio of 0.9 were obtained. However, a discharge duration close to the charging duration could not be obtained in this study.

There have also been some studies on the biomass gasification approach as a method for hydrogen production for clean environment. In one of these studies [36], the proposed system with SOFC for hydrogen production was analyzed for energy and exergy using the first and second law of thermodynamics. It was reported that a 16.68% improvement in thermal efficiency and a net power output of up to 8.0 MW was achieved with this proposed system.

In the studies in the literature, the performances of SOFCs have been investigated using different fuels. In addition, thermodynamic analyses were performed in combined power systems with these fuel cells and efficiency values were obtained. However, it is seen that these thermodynamic approaches are not reported in the studies conducted for performance analysis in the literature. In this research, the performance of the SOFC was evaluated under three different operating temperatures supported by energy and exergy analysis thermodynamically.

2. MATERIAL AND METHOD

A SOFC operating at high temperatures consists of three basic materials: anode, cathode and electrolyte, as shown in Figure 1. Similar to other fuel cells, the principle of operation in SOFC is the production of electricity as a result of electrochemical reactions between oxygen and fuel. The electrochemical processes result in the release of the fuel's electrons at the anode. Oxygen ions dissociate at the cathode and move through the electrolyte towards the anode, reacting with the fuel molecules. As a result of this reaction, oxygen combined with electrons forms byproducts and completes the energy generation.

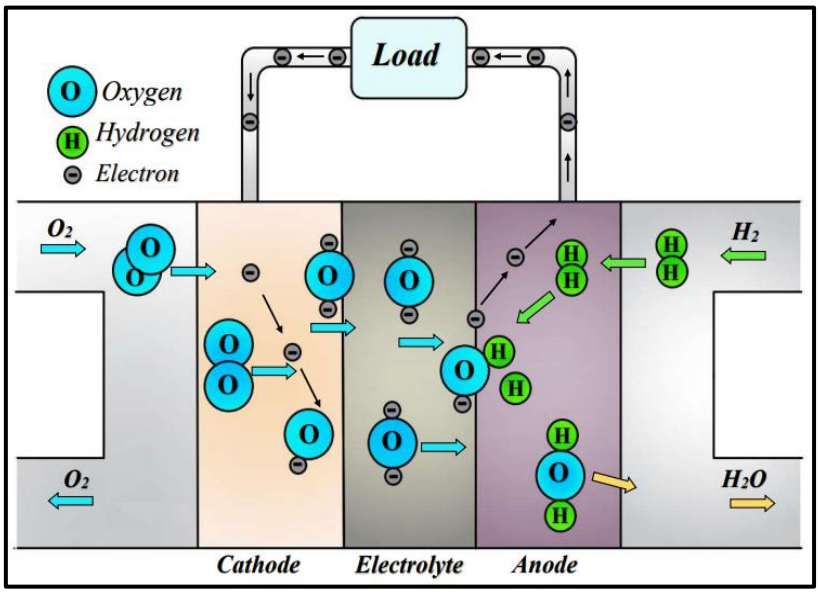

Figure 1. The SOFC's basic structure and working principle

When hydrogen reacts with oxygen in the anode and cathode regions of the fuel cell, water is formed. The released energy during this reaction leads to the generation of electricity at the electrodes. Reactions at the anode and cathode electrode:

$$H_2 \rightarrow 2H^+ + 2e^- \quad (1)$$

$$1/2\, O_2 + 2e^- \rightarrow O^{2-} \quad (2)$$

$$H_2 + 1/2\, O_2 \rightarrow H_2O + heat + electricity \quad (3)$$

Activation losses (η_{act}), concentration losses (η_{conc}) and ohmic losses (η_{ohmic}) are realized at the anode and cathode during energy production in SOFC. The cell voltage/potential is obtained by subtracting all losses in the cell from the equilibrium potential (*E*) of the cell. The calculation of the cell voltage (*V*) is quite important because this value represents the fuel cell's performance.

$$V = E - \eta_{act} - \eta_{conc} - \eta_{ohmic} \quad (4)$$

The equilibrium potential (*E*) is defined as the equilibrium state of the reactions in the system. This potential changes depending on the pressure of hydrogen, oxygen and water ($P_{H_2}, P_{O_2}\ and\ P_{H_2O}$) apart from the universal gas constant (*R*) and Faraday's constant (*F*). The reversible potential (E_0) given in Equation 6 is used to calculate the equilibrium potential [37]. The reversible potential is only affected by temperature (T).

$$E = E_0 + \frac{RT}{2F} \ln\left(\frac{P_{H_2} \cdot {P_{O_2}}^{1/2}}{P_{H_2O}}\right) \quad (5)$$

$$E_0 = 1.253 - 2.451 \times 10^{-4}\, T \quad (6)$$

The activation loss in SOFC is calculated from Equation 7 with the help of Butler-Volmer equation. The activation loss (η_{act}), is determined by using the operating temperature (*T*) and exchange current density (J_0) except for the constant parameters (*R*, *F*) [38]. There is a correlation between current density (*J*) and exchange current density (J_0). In this study, the electron number (*z*) and symmetric factor (α) are assumed to be 2 and 0.5, respectively [39].

$$J = J_0 \left[\exp\left(\frac{\alpha z F \eta_{act}}{RT}\right) - \exp\left(\frac{(1-\alpha) z F \eta_{act}}{RT}\right)\right] \quad (7)$$

$$\eta_{act,i} = \frac{RT}{F} sinh^{-1}\left(\frac{J}{2J_{0,i}}\right) \quad (8)$$

i = a, c

As shown in the equations below, the exchange current density (J_0) is calculated depending on the pressure (P) of the gases at the cathode and anode, except for the fixed parameters such as electrode porosity (n), pore diameter (D_p) and grain size (D_s) given in Tables 1 and 2 [39].

$$J_{0,a} = k_a \frac{72\times[D_p-(D_p+D_s)n]n}{{D_s}^2{D_p}^2(1-\sqrt{1-X^2})} \times \left(\frac{P_{H_2}}{P_{ref}}\right) \times \left(\frac{P_{H_2O}}{P_{ref}}\right) \times \exp\left(-\frac{E_{act,a}}{RT}\right) \quad (9)$$

$$J_{0,c} = k_c \frac{72\times[D_p-(D_p+D_s)n]n}{{D_s}^2{D_p}^2(1-\sqrt{1-\alpha^2})} \times \left(\frac{P_{O_2}}{P_{ref}}\right)^{0.25} \times \exp\left(-\frac{E_{act,c}}{RT}\right) \quad (10)$$

The concentration losses (η_{conc}) in SOFC are calculated in two different ways: at the anode and at the cathode. The concentration loss, causing energy loss, occurs in the process of diffusion of gases at the electrode. Fick's law of diffusion is used to calculate these losses. Fick's law describes how gases move along the electrode surface. The concentration losses at the anode and cathode are determined by the following equations [37,40,41]:

$$\eta_{conc,a} = \frac{RT}{2F} \ln\left[\frac{1+\frac{RTt_aJ}{2FD_a^{eff}P^0_{H_2O}}}{1-\frac{RTt_aJ}{2FD_a^{eff}P^0_{H_2}}}\right] \quad (11)$$

$$\eta_{conc,c} = \frac{RT}{2F} \ln\left[\frac{1}{1-J/J_{L,O_2}}\right] \quad (12)$$

$$J_{L,O_2} = \frac{zFD_c^{eff}}{RTt_c} p_{O_2} \quad (13)$$

$$\frac{1}{D_a^{eff}} = \frac{\xi}{n}\left(\frac{1}{D_{H_2-H_2O}} + \frac{1}{D_{H_2,k}}\right) \quad (14)$$

$$\frac{1}{D_c^{eff}} = \frac{\xi}{n}\left(\frac{1}{D_{O_2-N_2}} + \frac{1}{D_{O_2,k}}\right) \quad (15)$$

In a SOFC, ohmic losses (η_{ohmic}) affected by operating temperature (T), current density (J) and electrolyte thickness (t_e) are calculated as given in Equation 16 [42].

$$\eta_{ohmic} = 2.99 \times 10^{-11}.J.t_e\,.exp\left(\frac{10300}{T}\right) \quad (16)$$

Table 1. Inlet operating conditions [39]

Items	**Values**	**Unit**
Anode activation energy, $\boldsymbol{E_{act,a}}$	1.344 x 10^{10}	[J/mol]
Cathode activation energy, $\boldsymbol{E_{act,c}}$	2.051 x 10^{9}	[J/mol]
Temperature of operation, $\boldsymbol{T}$	973 - 1173	[K]
Pressure of operation, $\boldsymbol{P}$	1	[bar]
Faraday constant, $\boldsymbol{F}$	96485	[C/mol]
Universal gas constant, $\boldsymbol{R}$	8.3145	[J/mol K]

Table 2. SOFC system design parameters [39-43]

Items	**Values**	**Unit**
Active cell area, $\boldsymbol{A}$	0.0834	[m^2]
Anode thickness, $\boldsymbol{t_a}$	100	[µm]
Cathode thickness, $\boldsymbol{t_c}$	750	[µm]
Electrolyte thickness, $\boldsymbol{t_e}$	100	[µm]
Average pore radius, $\boldsymbol{D_p}$	2	[µm]
Average grain size, $\boldsymbol{D_s}$	1.5	[µm]
Anode's porosity, $\boldsymbol{n}$	0.48	–
Anode's tortuosity, $\boldsymbol{\xi}$	5.4	–
Average grain contact length, $\boldsymbol{X}$	0.7	–

The mass balance in the control volume of a SOFC is described by considering the movement of reactants and products in the cell. While hydrogen and oxygen enter the control volume, water and oxygen exit (Figure 2).

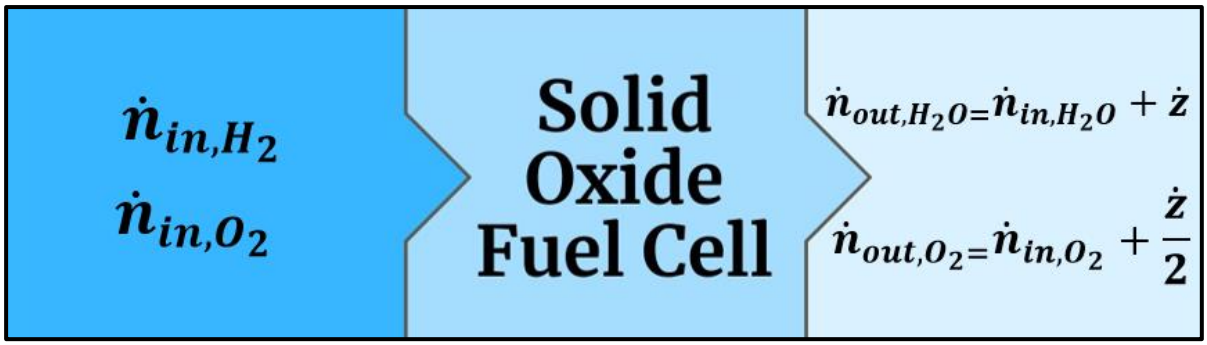

Figure 2. The control volume for the SOFC

The mass balance of reactants and products in the control volume of SOFC is given in the following equations [44]:

$$\dot{n}_{out,H_2}=\dot{n}_{in,H_2}-\dot{z} \quad (17)$$

$$\dot{n}_{out,H_2O}=\dot{n}_{in,H_2O}+\dot{z} \quad (18)$$

$$\dot{n}_{out,O_2}=\dot{n}_{in,O_2}+\frac{\dot{z}}{2} \quad (19)$$

$$\dot{n}_{out,N_2}=\dot{n}_{in,N_2} \quad (20)$$

The number of moles of hydrogen entering through the anode electrode in SOFC is denoted as $\dot{z}$. This value is calculated by multiplying the fuel utilization factor (U_f) and the molar flow rate ($\dot{n}$) [44].

$$\dot{z}=U_f\dot{n}_{in,H_2} \quad (21)$$

The molar flow rate of oxygen is determined by the ratio of the number of moles to the fuel utilization factor as given in Equation 22 [44].

$$\dot{n}_{in,O_2}=\frac{\dot{z}}{2U_f} \quad (22)$$

The thermal efficiency in SOFC is calculated as the ratio between the available energy ($\dot{W}_{FC}$) and the energy of the fuel used ($\dot{F}_{in}$).

$$\eta_{thermal} = \frac{\dot{W}_{FC}}{\dot{F}_{in}} \quad (23)$$

The energy balance in a fuel cell is expressed as follows [45,46].

$$\dot{Q} - \dot{W} = \sum_i \dot{n}_i \, \bar{h}_i - \sum_e n_e \, \bar{h}_e \quad (24)$$

Exergy is defined thermodynamically as the potential of a system to convert its internal energy into work that it can do for its environment. Exergy measures internal energy in terms of its capacity to do work and assesses the regularity and energy quality of the system. The exergy in a fuel cell includes the thermal, mechanical and chemical energy components of the system and determines the efficiency of the energy conversion process by reflecting the potential to efficiently convert these forms of energy into useful work. The system's exergy is obtained by summing the physical and chemical exergy (Equation 25) [47]. The exergy of SOFC varies depending on enthalpy and entropy according to the determined operating temperature.

$$E\dot{x} = E\dot{x}^{ph} + E\dot{x}^{ch} \quad (25)$$

$$E\dot{x}^{ph} = \sum_i \dot{n}_i \left(\bar{h}_i - \bar{h}_0\right) - T_0 \left(\bar{s}_i - \bar{s}_0\right) \quad (26)$$

$$E\dot{x}^{ch} = \dot{n}\left(\sum_i y_i \overline{ex}_i^{ch,0} + \bar{R} T_0 \sum_i y_i \ln y_i\right) \quad (27)$$

Exergy destruction is a term that refers to the loss of useful work in a fuel cell. Exergy destruction usually occurs due to energy losses from friction, heat transfer and irreversible processes in the cycle. Lower exergy destruction means higher efficiency of energy conversion. Entropy production and exergy destruction are calculated from the following equations:

$$\Delta E\dot{x}_{dest} = \left(E\dot{x}_{O_2} + E\dot{x}_{H_2}\right) - \left(P + E\dot{x}_{out,\ O_2} + E\dot{x}_{out,\ H_2O}\right) \quad (28)$$

$$\Delta S = \frac{\Delta E\dot{x}_{dest}}{T_0} \quad (29)$$

As given in Equation 30, exergy efficiency is described as the proportion of system's available energy to the input exergy. Exergy efficiency includes the amount of losses, i.e. higher exergy efficiency means that energy is used more efficiently with less losses [47].

$$\eta_{exergy} = \frac{\dot{W}_{FC}}{E\dot{x}_{in}} \times 100 \quad (30)$$

3. RESULTS AND DISCUSSION

The objective of this research is to examine the performance of a SOFC via a pore diameter of 2 μm at operating temperatures of 973 K, 1073 K and 1173 K. In the scope of the study, the activation, concentration and ohmic losses affecting the SOFC performance were determined and the voltage of the cell was calculated at different operating conditions. Power density, exergy destruction, entropy production, thermal and exergy efficiency were also determined. The influence of CD and temperature variation on concentration and ohmic losses in SOFC is given in Figures 3 and 4. The concentration losses in the cell tend to rise with increasing temperature. The limit CD is the main factor in determining the concentration losses. Decreasing the operating temperature increases the limit CD. The limit CD at the cathode increased by 15.81% as the temperature decreased from 1073 K to 973 K. The concentration losses at 1173 K and 973 K operating temperatures were 0.0081 V and 0.0049 V, respectively, at constant CD condition in SOFC. Each 100 K increase in the temperature of the cell increased the concentration losses by 24.91% on average under constant conditions. The activation loss in the cell was calculated as 0.00445 V at a CD of 3500 A/m^2 and 1073 K operating temperature. In addition, the concentration loss also showed an increase with rising CD. The variation of the CD from 2000 A/m^2 to 4000 A/m^2 at the same operating temperature increased the concentration loss in the cell by 99.35%. Ni et al. [39] designed a model to analyze the performance of a SOFC. According to the data obtained, the increase in operating temperature negatively affected the concentration loss. Under constant current density, the concentration loss increased from 0.13 V at 873 K operating temperature to 0.2 V at 1273 K.

Ohmic losses occurring during the operation of the SOFC have a lower magnitude compared to other types of losses. However, a detailed study of all loss mechanisms is an important requirement to determine the most effective operating conditions of SOFC. Ohmic losses occur due to resistance during the conduction of electric current and are often less obvious compared to other types of losses. The thickness of electrolyte, CD and cell temperature are the main

effective parameters in the determination of ohmic losses. The ohmic losses are 5.32×10^{-7} V and 8.75×10^{-8} V at operating temperatures of 973 K and 1173 K, respectively at a CD of 4500 A/m^2. The ohmic losses increased by 83.55% with a decrease in temperature by 200 K at constant CD. Heidarshenas et al. [48] investigated the performance of a SOFC by exergy and energy analysis. The results showed that increasing the operating temperature significantly decreased the ohmic losses. The ohmic losses for operating temperatures of 800°C and 1100°C were 0.25 V and 0.04 V, respectively, at an operating pressure of 3 bar.

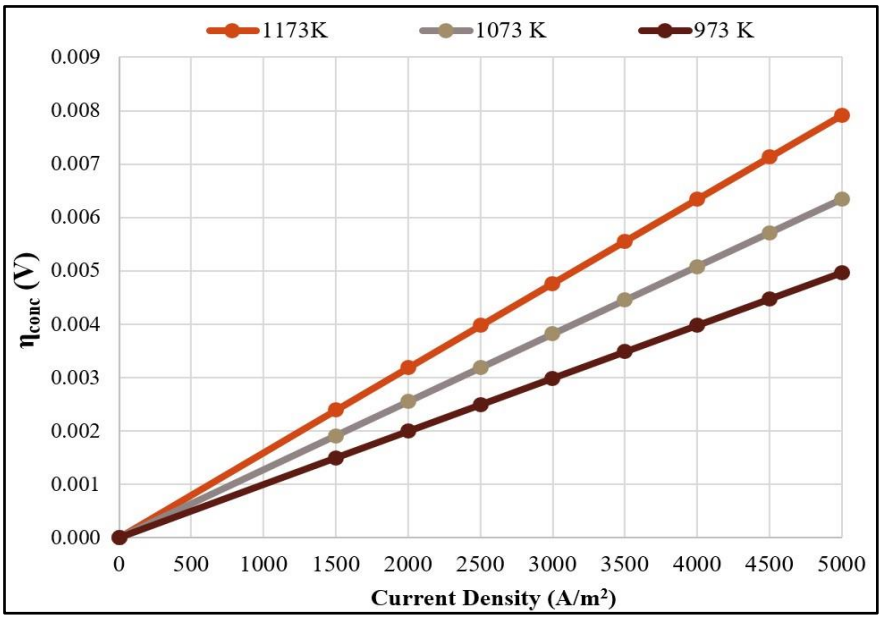

Figure 3. The concentration cell loss at various operating temperatures in a SOFC

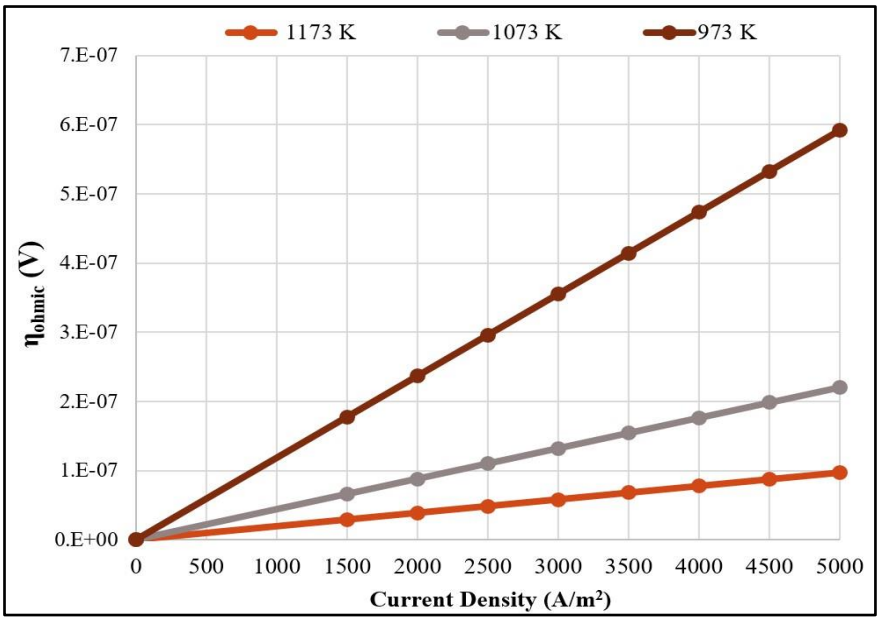

Figure 4. The ohmic cell loss at various operating temperatures in a SOFC

The increasing voltage values of the SOFC with respect to temperature are mainly due to electrochemical reactions are strongly related to temperature. High temperatures increase the rate of electrochemical reactions between the anode and cathode, allowing the transport of electrons and ions. The combination of these factors provides the high cell potential and maximum power density of SOFC. Power density refers to the amount of electrical energy generated depending on the surface area in the cell.

The variation of cell potential and power density with respect to temperature is seen in Figure 5 and Figure 6, respectively. If the CD is kept constant when the temperature is rose from 973 K to 1073 K, there is an increase of 35.04% in the cell potential and power density. Also, at a constant temperature, while the cell voltage is 0.9690 V at a CD of 2000 A/m^2, this value decreases to 0.8197 V at a CD of 4500 A/m^2. The cell voltage is 0.64 V and the power density is 1927.17 W/m^2 at a CD of 3500 A/m^2 and 973 K operating temperature. Moreover, the maximum power density is calculated as 1587.67 W/m^2 at 1173 K operating temperature. Ni et al. [39] analyzed the performance of SOFC fuel cell at four different temperatures: 873 K, 973 K, 1073 K and 1273 K. As the temperature of the cell decreased, the cell potential also decreased. Under constant current density, the cell voltage was 0.08 V at 873 K operating temperature and 0.7 V at 1073 K operating temperature. The power density also showed a similar trend with the cell potential. The maximum power density was determined as 1.5 W/cm^2 at 1273 K operating temperature.

Ran et al. [49] analyzed the performance of a SOFC fuel cell hybrid system. The cell potential decreased with increasing CD. For current densities of 4800 A/m^2 and 5500 A/m^2, the cell potential became 0.65 V and 0.61 V, respectively.

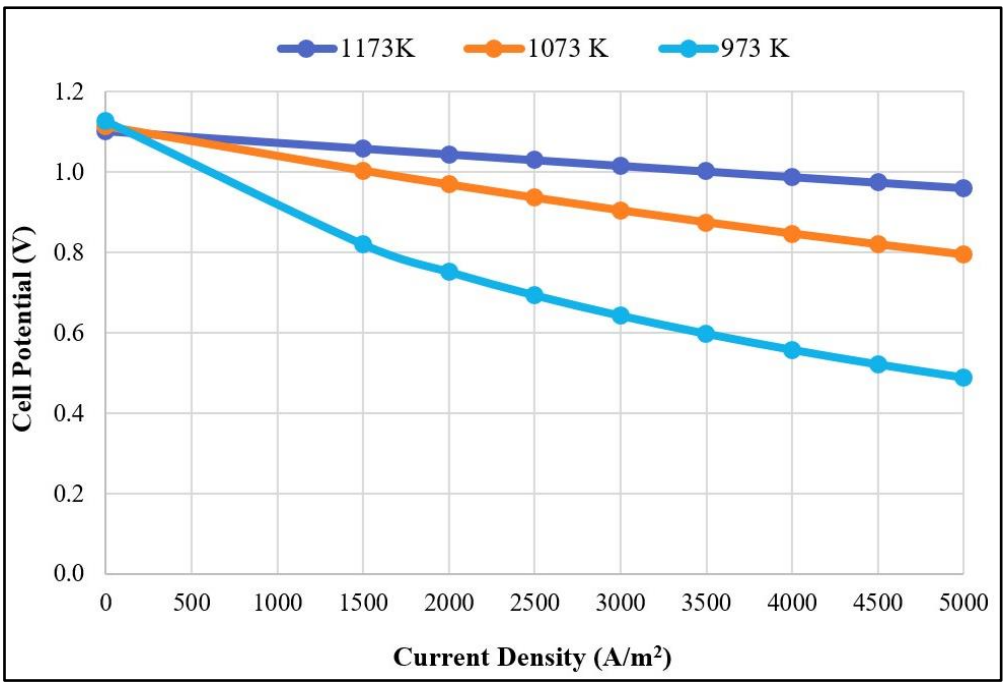

Figure 5. The cell potential at various operating temperatures in a SOFC

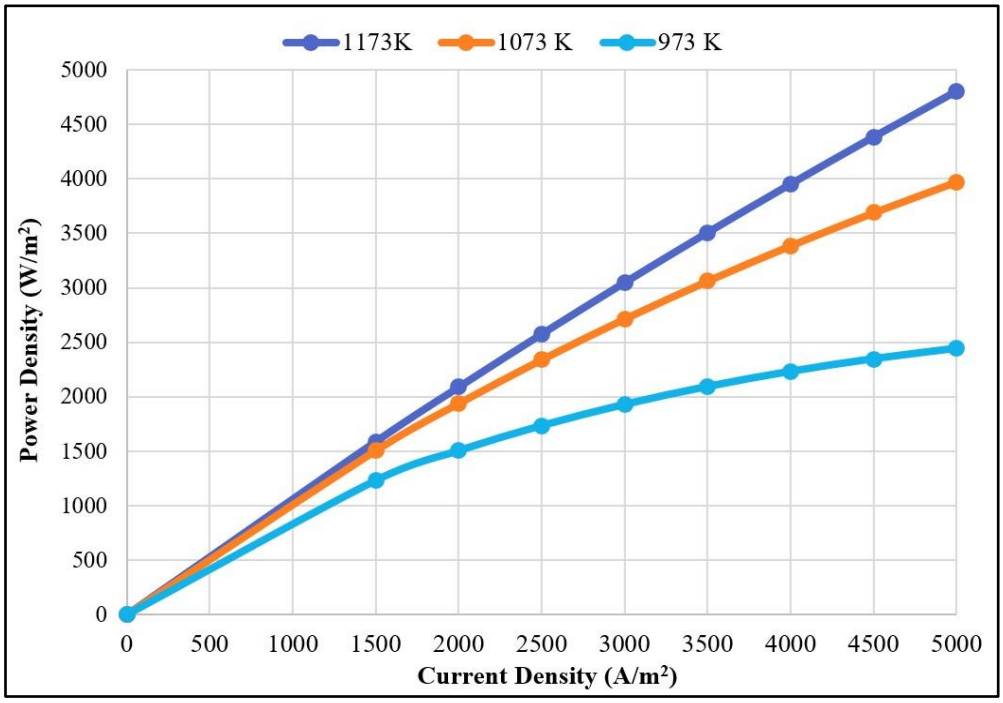

Figure 6. The power density at various operating temperatures in a SOFC

The exergy loss and entropy production in a SOFC are thermodynamically defined as energy losses and increase in irregularity in the system. The exergy destruction in SOFC includes losses due to heat transfer, internal resistances and chemical reactions that occur during the energy

utilization processes in the cell. Entropy production indicates the irregularity of the system and the more complex distribution of energy as a result of these processes.

Figures 7 and 8 show the effect of various operating temperatures on exergy destruction and entropy production. The amount of exergy destruction and entropy production decreased with increasing temperature in the cell. The max. exergy destruction and entropy production in SOFC were observed at 973 K, which is the lowest operating temperature. Under constant CD, these values are 1147.01 kW and 3.85 kW/K, respectively. If the temperature of operation is rose from 973 K to 1173 K while the CD is kept constant, the SOFC's exergy destruction decreases by 38.15%. The calculated exergy destruction is 3944.39 kW and entropy production is 13.24 kW/K at a CD of 5000 A/m^2 and 1073 K operating temperature. Heidarshenas et al. [48] investigated the performance of a system integrated with SOFC fuel cell by thermodynamic analysis. The increase of the operating temperature and pressure up to the optimum point had a positive effect on the power of the SOFC and caused a decrease in the exergy destruction. The exergy destruction of the SOFC was calculated as 0.32 kW.

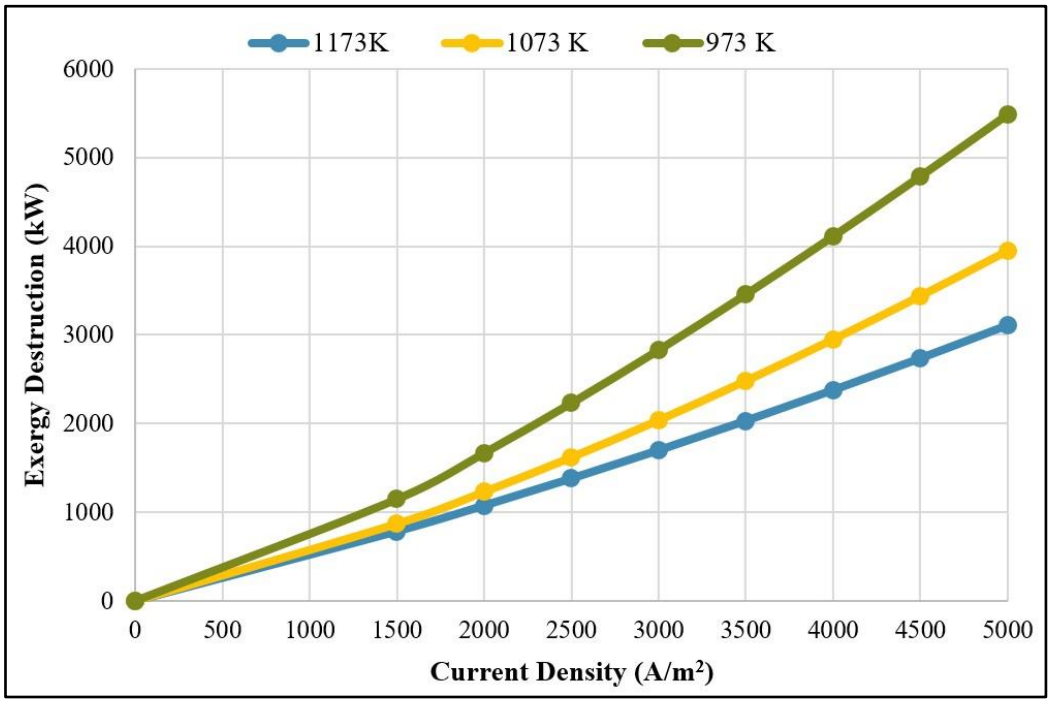

Figure 7. The exergy destruction at various operating temperatures in a SOFC

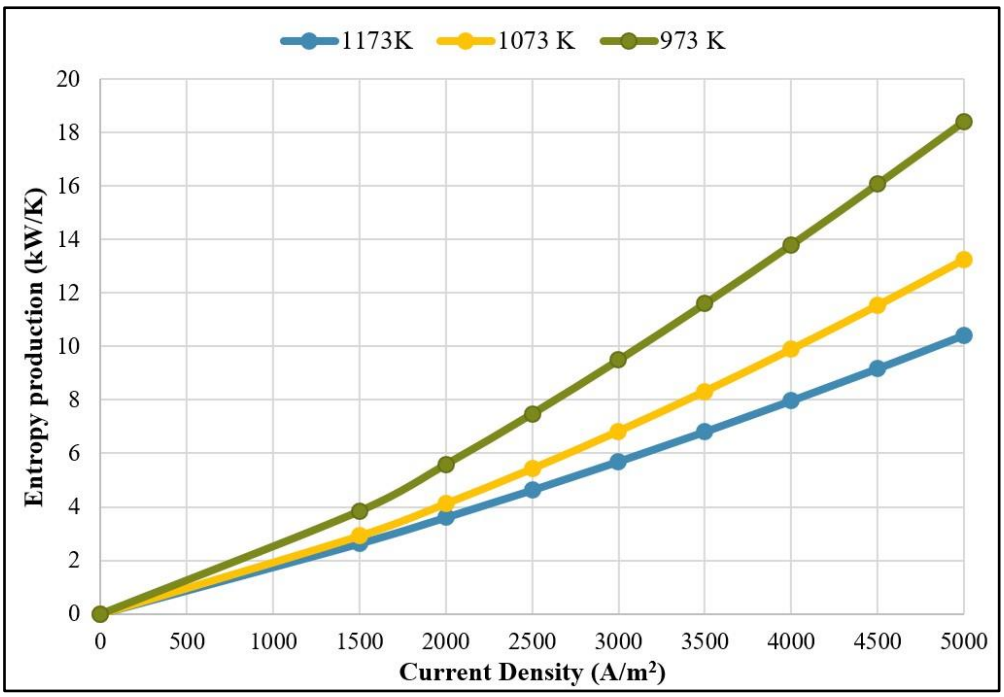

Figure 8. The entropy production at various operating temperatures in a SOFC

In a SOFC, thermal and exergy efficiencies refer to the thermodynamic measurement of performance. The effect of operating temperature on thermal and exergy efficiencies is demonstrated in Table 3. The thermal efficiency shows the capacity of the cell to convert heat energy into electrical energy. Thermal efficiency varies depending on the potential of the cell and hence the power density. The exergy efficiency includes factors related to exergy losses and irregularities in the cell and evaluates the energy conversion process efficiency of the cell. These two efficiencies are very important to understand and optimize the efficiency of energy conversion for SOFC. The maximum efficiency in the system indicates that the cell operates more effectively and utilizes energy resources more efficiently.

The thermal and exergy efficiency increased in direct proportion to the increase in operating temperature in SOFC. The maximum thermal and exergy efficiencies were calculated at a temperature of 1173 K and a CD of 1500 A/m^2 . These efficiency values are 71.34% and 66.93% respectively. The thermal efficiency is 60.97% and the exergy efficiency is 57.14% at a CD of 3000 A/m^2 and an operating temperature of 1073 K. Yang et al. [50] conducted an exergy and exergoeconomic analysis of a SOFC system. As the operating temperature higher, the exergy efficiency increased up to the optimum point. At 750°C and 850°C, the exergy efficiencies were

35.4% and 38.7%, respectively. The maximum exergy efficiency of SOFC was calculated as 40% at 950°C operating temperature.

The thermal efficiency and exergy efficiency were negatively affected by 12.39% and 11.62%, respectively, by tripling the CD at constant temperature. Zhang et al. [51] conducted computations to understand the effect of various operating parameters such as current density, temperature, electrode porosity and thickness on the performance of SOFC. With in the scope of the results obtained, it was seen that the increase in current density caused a decrease in energy efficiency. A 50% increase in CD of decreased the energy yield by approximately 15% compared to the initial case.

Table 3. The thermal and exergy efficiency at different operating temperatures in a SOFC

Current Density (A/m^2)	Thermal Efficiency (%)			Exergy Efficiency (%)		
	1173 K	1073 K	973 K	1173 K	1073 K	973 K
1500	71.35	67.66	55.28	66.93	63.40	51.75
2000	70.38	65.32	50.66	66.03	61.21	47.42
2500	69.42	63.10	46.72	65.13	59.12	43.74
3000	68.47	60.98	43.30	64.23	57.14	40.53
3500	67.53	58.97	40.28	63.35	55.26	37.71
4000	66.59	57.07	37.58	62.47	53.47	35.18
4500	65.67	55.26	35.14	61.61	51.78	32.89
5000	64.76	53.55	32.91	60.75	50.17	30.81

4. CONCLUSIONS

In this study, the effects of three various operating temperatures (973 K, 1073 K and 1173 K) were investigated by detailed calculations to assess the performance of a cathode supported SOFC. The SOFC model analyzed has a cathode thickness of 750 μm, a pore diameter of 2 μm and an active cell area of 0.0834 m^2. Firstly, the losses occurring in the cell were calculated to

determine the cell potential. While activation and ohmic losses decreased with increasing temperature, concentration losses increased as can be seen in Figure 3. Therefore, it is very important to choose the appropriate temperature in SOFC. The cell voltage and power density of the SOFC were calculated as 0.87 V and 3061.87 W/m^2, respectively, at a CD of 3500 A/m^2 and an operating temperature of 1073 K. It was observed that an increment of 100 K in the operating temperature increased the power density by up to 1.62 times at constant CD. The exergy destruction, entropy production, thermal and exergy efficiencies were calculated by performing energy and exergy analysis. Table 3 shows the effect of various operating temperatures on thermal efficiency and exergy efficiency. It can be clearly seen from the table that the thermal efficiency increases with increasing temperature. At the same current density condition, the thermal efficiency at 973 K operating temperature was 46.72%, while at 1173 K the thermal efficiency was 69.42%. According to the obtained results, it can be seen that the maximum exergy efficiency depends on the min. exergy destruction in SOFC. Figure 7 shows the exergy destruction due to current density at various temperatures. As the operating temperature decreases, the exergy loss increases. The main reason for this is the high cell losses at low operating temperatures. At an operating temperature of 1173 K and a current density of 2500 A/m^2, the minimum exergy loss in the fuel cell was 1378.68 kW. The exergy efficiency calculated using this exergy destruction was determined as 65.13%.

DECLARATION OF ETHICAL STANDARDS

The authors of the paper submitted declare that nothing which is necessary for achieving the paper requires ethical committee and/or legal-special permissions.

CONFLICT OF INTEREST

There is no conflict of interest in this study.

CONTRIBUTION OF THE AUTHORS

Serdar Halis: Conceptualization, Writing-original draft, Visualization, Review and editing, Methodology.

Nisa Nur Atak: Writing-original draft, Visualization, Review and editing.

Battal Doğan: Conceptualization, Methodology, Writing-original draft, Supervision.

REFERENCES

[1] Panwar NL, Kaushik SC, Kothari S. Role of renewable energy sources in environmental protection: A review. Renewable and Sustainable Energy Reviews 2011;15:1513–1524.

[2] Al-Hamed KH, Dincer I. A novel ammonia solid oxide fuel cell-based powering system with on-board hydrogen production for clean locomotives. Energy 2021;220:119771.

[3] Abe JO, Popoola API, Ajenifuja E, Popoola OM. Hydrogen energy, economy and storage: Review and recommendation. International Journal of Hydrogen Energy 2019;44:15072–86.

[4] Du Y, Yang Z, Hou Y, Lou J, He G. Part-load performance prediction of a novel diluted ammonia-fueled solid oxide fuel cell and engine combined system with hydrogen regeneration via data-driven model. Journal of Cleaner Production 2023;395:136305.

[5] Meng T, Cui D, Ji Y, Cheng M, Tu B, Lan Z. Optimization and efficiency analysis of methanol SOFC-PEMFC hybrid system. International Journal of Hydrogen Energy 2022;47:27690–702.

[6] Da Silva AAA, Steil MC, Tabuti FN, Rabelo-Neto RC, Noronha FB, Mattos LV, et al. The role of the ceria dopant on Ni/doped-ceria anodic layer cermets for direct ethanol solid oxide fuel cell. International Journal of Hydrogen Energy 2021;46:4309–28.

[7] Yu F, Han T, Wang Z, Xie Y, Wu Y, Jin Y, et al. Recent progress in direct carbon solid oxide fuel cell: Advanced anode catalysts, diversified carbon fuels, and heat management. International Journal of Hydrogen Energy 2021;46:4283–300.

[8] Cimenti M, Hill JM. Direct utilization of liquid fuels in SOFC for portable applications: challenges for the selection of alternative anodes. Energies 2009;2:377–410.

[9] Acar C, Dincer I. The potential role of hydrogen as a sustainable transportation fuel to combat global warming. International Journal of Hydrogen Energy 2020;45:3396–406.

[10] Boldrin P, Ruiz-Trejo E, Mermelstein J, Bermúdez Menéndez JM, Ramírez Reina T, Brandon NP. Strategies for Carbon and Sulfur Tolerant Solid Oxide Fuel Cell Materials, Incorporating Lessons from Heterogeneous Catalysis. Chem Rev 2016;116:13633–84.

[11] Ge X, Chan S, Liu Q, Sun Q. Solid Oxide Fuel Cell Anode Materials for Direct Hydrocarbon Utilization. Advanced Energy Materials 2012;2:1156–81.

[12] Prakash BS, Kumar SS, Aruna ST. Properties and development of Ni/YSZ as an anode material in solid oxide fuel cell: A review. Renewable and Sustainable Energy Reviews 2014;36:149–79.

[13] Palomba V, Ferraro M, Frazzica A, Vasta S, Sergi F, Antonucci V. Experimental and numerical analysis of a SOFC-CHP system with adsorption and hybrid chillers for telecommunication applications. Applied Energy 2018;216:620–33.

[14] Kirubakaran A, Jain S, Nema RK. A review on fuel cell technologies and power electronic interface. Renewable and Sustainable Energy Reviews 2009;13:2430–40.

[15] Kariya T, Tanaka H, Hirono T, Kuse T, Yanagimoto K, Uchiyama K, et al. Development of a novel cell structure for low-temperature SOFC using porous stainless steel support combined with hydrogen permeable Pd layer and thin film proton conductor. Journal of Alloys and Compounds 2016;654:171–5.

[16] Gong M, Liu X, Trembly J, Johnson C. Sulfur-tolerant anode materials for solid oxide fuel cell application. Journal of Power Sources 2007;168:289–98.

[17] Bossel U. Rapid startup SOFC modules. Energy Procedia 2012;28:48–56.

[18] Zhang L, Chen G, Dai R, Lv X, Yang D, Geng S. A review of the chemical compatibility between oxide electrodes and electrolytes in solid oxide fuel cells. Journal of Power Sources 2021;492:229630.

[19] Zakaria Z, Kamarudin SK. Advanced modification of scandia-stabilized zirconia electrolytes for solid oxide fuel cells application—A review. Int J Energy Res 2021;45:4871–87.

[20] Ma M, Yang X, Qiao J, Sun W, Wang Z, Sun K. Progress and challenges of carbon-fueled solid oxide fuel cells anode. Journal of Energy Chemistry 2021;56:209–22.

[21] Jiang Y, Chen F, Xia C. A review on cathode processes and materials for electro-reduction of carbon dioxide in solid oxide electrolysis cells. Journal of Power Sources 2021;493:229713.

[22] Cao J, Su C, Ji Y, Yang G, Shao Z. Recent advances and perspectives of fluorite and perovskite-based dual-ion conducting solid oxide fuel cells. Journal of Energy Chemistry 2021;57:406–27.

[23] Barelli L, Bidini G, Cinti G, Ottaviano PA. Solid oxide fuel cell systems in hydrogen-based energy storage applications: Performance assessment in case of anode recirculation. Journal of Energy Storage 2022;54:105257.

[24] Dincer I. Green methods for hydrogen production. International Journal of Hydrogen Energy 2012;37:1954–71.

[25] Posdziech O, Schwarze K, Brabandt J. Efficient hydrogen production for industry and electricity storage via high-temperature electrolysis. International Journal of Hydrogen Energy 2019;44:19089–101.

[26] Kazempoor P, Dorer V, Ommi F. Evaluation of hydrogen and methane-fuelled solid oxide fuel cell systems for residential applications: System design alternative and parameter study. International Journal of Hydrogen Energy 2009;34:8630–44.

[27] Cinti G, Bidini G, Hemmes K. Comparison of the solid oxide fuel cell system for micro CHP using natural gas with a system using a mixture of natural gas and hydrogen. Applied Energy 2019:238, 69-77. https://doi.org/10.1016/j.apenergy.2019.01.039.

[28] Jia J, Abudula A, Wei L, Sun B, Shi Y. Thermodynamic modeling of an integrated biomass gasification and solid oxide fuel cell system. Renewable Energy 2015;81:400–10.

[29] Papurello D, Lanzini A, Tognana L, Silvestri S, Santarelli M. Waste to energy: Exploitation of biogas from organic waste in a 500 Wel solid oxide fuel cell (SOFC) stack. Energy 2015;85:145–58.

[30] Gandiglio M, Lanzini A, Santarelli M, Leone P. Design and balance-of-plant of a demonstration plant with a solid oxide fuel cell fed by biogas from waste-water and exhaust carbon recycling for algae growth. Journal of Fuel Cell Science and Technology 2014;11:031003.

[31] Leone P, Lanzini A, Ortigoza-Villalba GA, Borchiellini R. Operation of a solid oxide fuel cell under direct internal reforming of liquid fuels. Chemical Engineering Journal 2012;191:349–55.

[32] Cocco D, Tola V. Externally reformed solid oxide fuel cell–micro-gas turbine (SOFC–MGT) hybrid systems fueled by methanol and di-methyl-ether (DME). Energy 2009;34:2124–30.

[33] Jamsak W, Assabumrungrat S, Douglas PL, Croiset E, Laosiripojana N, Suwanwarangkul R, et al. Performance assessment of bioethanol-fed solid oxide fuel cell system integrated with distillation column. ECS Transactions 2007;7:1475.

[34] Baniasadi E, Dincer I. Energy and exergy analyses of a combined ammonia-fed solid oxide fuel cell system for vehicular applications. International Journal of Hydrogen Energy 2011;36:11128–36.

[35] Jienkulsawad P, Patcharavorachot Y, Chen Y-S, Arpornwichanop A. Energy and exergy analyses of a hybrid system containing solid oxide and molten carbonate fuel cells, a gas turbine, and a compressed air energy storage unit. International Journal of Hydrogen Energy 2021;46:34883–95.

[36] Zhou Y, Han X, Wang D, Sun Y, Li X. Optimization and performance analysis of a near-zero emission SOFC hybrid system based on a supercritical CO2 cycle using solar energy. Energy Conversion and Management 2023;280:116818.

[37] Chan SH, Khor KA, Xia ZT. A complete polarization model of a solid oxide fuel cell and its sensitivity to the change of cell component thickness. Journal of Power Sources 2001;93:130–40.

[38] Akikur RK, Saidur R, Ping HW, Ullah KR. Performance analysis of a co-generation system using solar energy and SOFC technology. Energy Conversion and Management 2014;79:415–30.

[39] Ni M, Leung MK, Leung DY. Parametric study of solid oxide fuel cell performance. Energy Conversion and Management 2007;48:1525–35.

[40] Chan SH, Ho HK, Tian Y. Multi-level modeling of SOFC–gas turbine hybrid system. International Journal of Hydrogen Energy 2003;28:889–900.

[41] Chan SH, Xia ZT. Polarization effects in electrolyte/electrode-supported solid oxide fuel cells. Journal of Applied Electrochemistry 2002;32:339–47.

[42] Ferguson JR, Fiard JM, Herbin R. Three-dimensional numerical simulation for various geometries of solid oxide fuel cells. Journal of Power Sources 1996;58:109–22.

[43] Liu Z, Tao T, Deng C, Yang S. Proposal and analysis of a novel CCHP system based on SOFC for coalbed methane recovery. Energy 2023;283:128996.

[44] Akkaya AV. Performance analysis of solid oxide fuel cell based energy generation systems with alternative criteria. PhD Thesis, Yıldız Technical University, 2007.

[45] Sadeghi M, Jafari M, Hajimolana YS, Woudstra T, Aravind PV. Size and exergy assessment of solid oxide fuel cell-based H2-fed power generation system with alternative electrolytes: A comparative study. Energy Conversion and Management 2021;228:113681.

[46] Sadeghi M, Nemati A, Yari M. Thermodynamic analysis and multi-objective optimization of various ORC (organic Rankine cycle) configurations using zeotropic mixtures. Energy 2016;109:791–802.

[47] Ranjbar F, Chitsaz A, Mahmoudi SMS, Khalilarya S, Rosen MA. Energy and exergy assessments of a novel trigeneration system based on a solid oxide fuel cell. Energy Conversion and Management 2014;87:318–27.

[48] Heidarshenas B, Abdullah MM, Sajadi SM, Yuan Y, Malekshah EH, Aybar HS. Exergy and environmental analysis of SOFC-based system including reformers and heat recovery

approaches to establish hydrogen-rich streams with least exergy loss. International Journal of Hydrogen Energy 2024;52:845-853.

[49] Ran P, Ou Y, Zhang C, Chen Y. Energy, exergy, economic, and life cycle environmental analysis of a novel biogas-fueled solid oxide fuel cell hybrid power generation system assisted with solar thermal energy storage unit. Applied Energy 2024;358:122618.

[50] Yang S, Wang G, Liu Z, Deng C, Xie N. Energy, exergy and exergo-economic analysis of a novel SOFC based CHP system integrated with organic Rankine cycle and biomass co-gasification. International Journal of Hydrogen Energy 2024;53:1155-1169.

[51] Zhang H, Li J, Xue Y, Grgur BN, Li J. Performance prediction and regulation of a tubular solid oxide fuel cell and hydrophilic modified tubular still hybrid system for electricity and freshwater cogeneration. Energy 2024;289:129893.